

## Ferromagnetism and spinodal decomposition in dilute magnetic nitride semiconductors

This article has been downloaded from IOPscience. Please scroll down to see the full text article.

2007 J. Phys.: Condens. Matter 19 365212

(<http://iopscience.iop.org/0953-8984/19/36/365212>)

View [the table of contents for this issue](#), or go to the [journal homepage](#) for more

Download details:

IP Address: 129.252.86.83

The article was downloaded on 29/05/2010 at 04:37

Please note that [terms and conditions apply](#).

# Ferromagnetism and spinodal decomposition in dilute magnetic nitride semiconductors

**K Sato, T Fukushima and H Katayama-Yoshida**

Institute of Scientific and Industrial Research, Osaka University, 8-1 Mihogaoka, Ibaraki, Osaka 567-0047, Japan

E-mail: [ksato@cmp.sanken.osaka-u.ac.jp](mailto:ksato@cmp.sanken.osaka-u.ac.jp)

Received 11 December 2006, in final form 1 February 2007

Published 24 August 2007

Online at [stacks.iop.org/JPhysCM/19/365212](http://stacks.iop.org/JPhysCM/19/365212)

## Abstract

We propose a materials design for dilute magnetic semiconductors (DMS) based on first-principles calculations by using the Korringa–Kohn–Rostoker coherent potential approximation method. We develop an accurate method for calculations of the Curie temperature ( $T_C$ ) of DMS and show that the mean field approximation completely fails to predict  $T_C$  for DMS, in particular for wide gap nitride DMS where the exchange interaction is short ranged. The  $T_C$  calculated for homogeneous DMS by using the present method agrees very well with available experimental values. For more realistic material design, we simulate spinodal nanodecomposition by applying the Monte Carlo method to the Ising model with *ab initio* chemical pair interactions between magnetic impurities in DMS. It is found that by controlling the dimensionality of the decomposition, various characteristic phases occur in DMS. It is suggested that superparamagnetic blocking phenomena should be important for understanding the magnetism of wide gap DMS.

## 1. Introduction

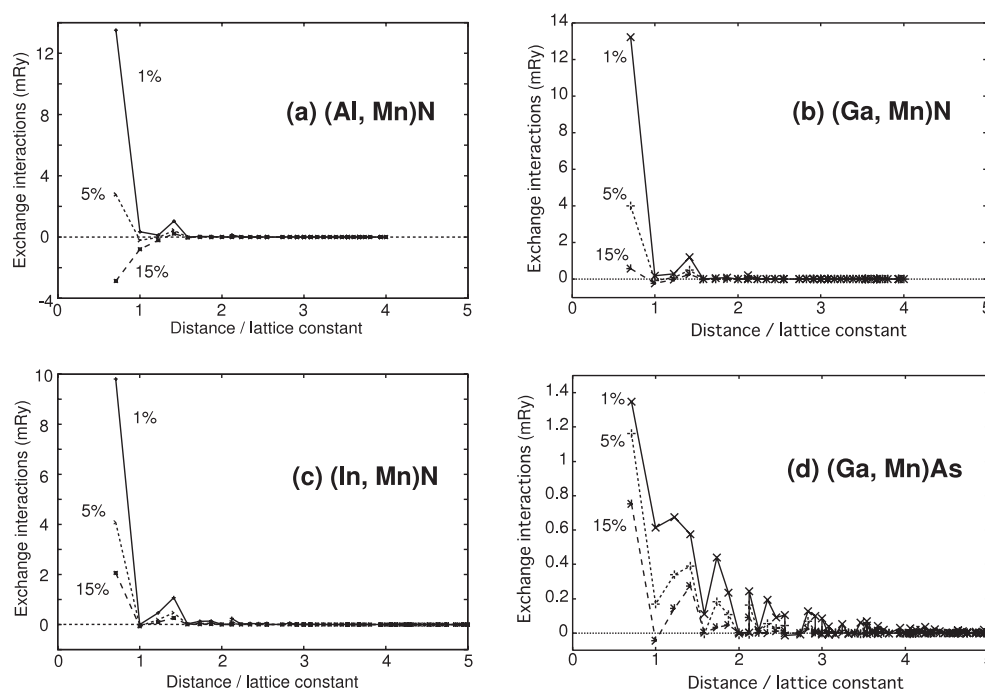
Dilute magnetic semiconductors (DMS) are recognized as being among the important materials for realizing semiconductor spintronics [1]. Already, many theories have been proposed for predicting magnetic properties of DMS [2–4]. Today, it has become possible to reproduce experimental Curie temperatures ( $T_C$ ) of DMS such as (Ga, Mn)As and (Zn, Cr)Te accurately from first principles [5–7]. In contrast to this success, agreement between the theory and experimental values is not satisfactory for wide band gap DMS such as nitride DMS, and a more realistic description of wide band gap DMS is needed. For example, in general, DMS systems have a solubility gap in thermal equilibrium and they show phase separation (spinodal decomposition); however in the previous theoretical approaches, homogeneous impurity distribution is supposed.

In this paper, we focus on the spinodal decomposition in nitride DMS, such as (Ga, Mn)N, (Ga, Cr)N and (Zn, Cr)Te, and study how the inhomogeneous impurity distribution affects the ferromagnetism. Magnetic and chemical pair interactions are calculated from first principles and the spinodal decomposition of DMS is simulated by applying the Monte Carlo method [8, 9].  $T_C$  for simulated spinodal decomposition phases is calculated within the random phase approximation, taking disorder into account [10, 11]. It will be shown that above the percolation threshold, the system is ferromagnetic and  $T_C$  goes up during the decomposition process in wide gap DMS [8]. For low concentrations, the system is superparamagnetic (i.e.  $T_C = 0$ ), because small isolated clusters are formed in DMS due to the decomposition. However, the Monte Carlo simulation for the magnetization process of the decomposition phases indicates that the superparamagnetic blocking temperature could be high because the activation energy of flipping the magnetization becomes large for the decomposition phases. Finally, we will take into account a layer-by-layer crystal growth condition in our simulations and will show that under this condition, quasi-one-dimensional nanostructures of impurities are formed in DMS even for low concentrations [9]. This simulation explains the ferromagnetic behaviour of wide gap DMS at high temperature.

## 2. Hybrid method for finding $T_C$ for DMS

For Curie temperature calculations, we employ a hybrid method to calculate the magnetic properties of DMS [5–7]. In the method, first we calculate the electronic structure of DMS by using the KKR-CPA (Korringa–Kohn–Rostoker coherent potential approximation) method [12, 13] and then effective exchange interactions are calculated assuming a classical Heisenberg model for the DMS. The exchange interactions  $J_{ij}$  are efficiently calculated by utilizing the magnetic force theorem. As Liechtenstein *et al* proposed [14], we calculate total energy change due to infinitesimal rotations of the two magnetic moments embedded at sites  $i$  and  $j$  in the effective CPA medium. The total energy change is mapped on the classical Heisenberg model to deduce the effective exchange interactions. Once the effective exchange interactions are calculated, we can use a standard statistical method for addressing the finite temperature magnetism. For example, the Curie temperature is calculated in the mean field approximation (MFA) or the random phase approximation (RPA) [15, 16]. By performing Monte Carlo simulation (MCS) we can exclude any approximations in  $T_C$  calculations [5, 6]. The MCS gives in principle the exact  $T_C$  for the model within statistical error. A similar method has been applied not only to DMS systems [17–19] but also to dilute magnetic oxides [20], Heusler alloys [21] and the other ferromagnets [22].

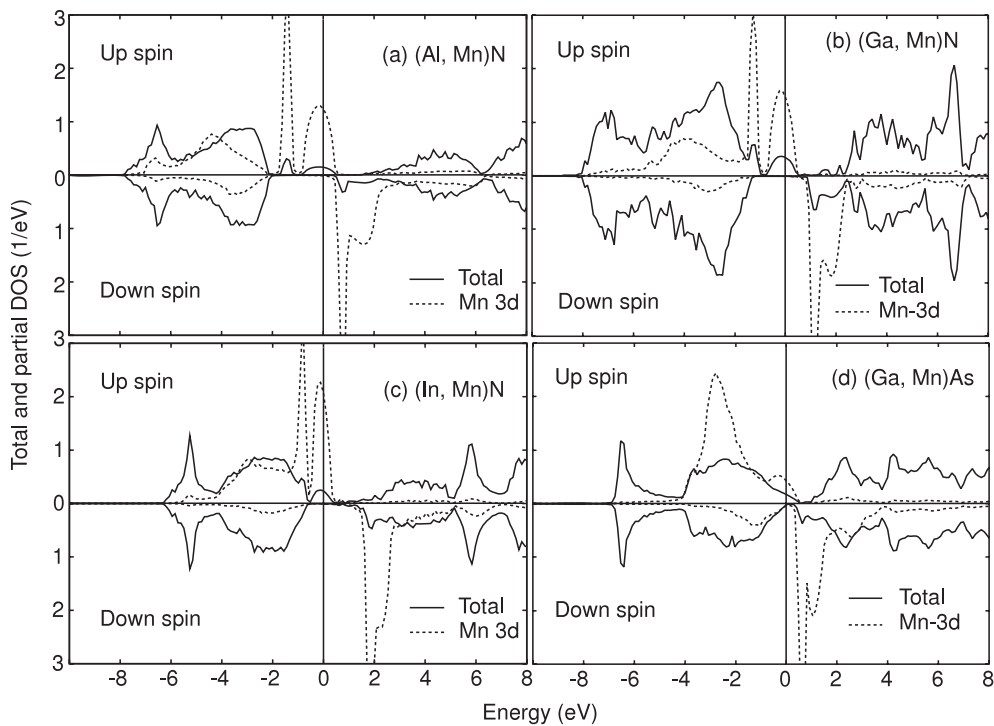
Figure 1 shows calculated effective exchange interactions in (Al, Mn)N, (Ga, Mn)N, (In, Mn)N and (Ga, Mn)As as a function of distance. The magnetic impurity concentrations are 1, 5 and 15%. For simplicity of calculation, we suppose the zinc blende crystal structure for GaN DMS. Lattice constants listed in [23] are used in the present calculations. It is found that in nitride DMS, the exchange interaction is characterized by very large nearest neighbour interaction and exponential decay of the interactions in the distance dependence. This is a typical behaviour of the exchange interactions in the DMS where magnetic impurities induce a deep impurity band in the band gap and the double exchange dominates [6, 5]. In fact, as shown in figures 2(a)–(c), calculated densities of states (DOS) in (Al, Mn)N, (Ga, Mn)N and (In, Mn)N show clear impurity bands in the gap. On the other hand, in (Ga, Mn)As (figure 2(d)), the Mn d states are far below the Fermi level and form a localized moment. This is nearly the electronic structure assumed in the p–d exchange model [24, 3]. Correspondingly, the exchange interactions are longer ranged as shown in figure 1(d).



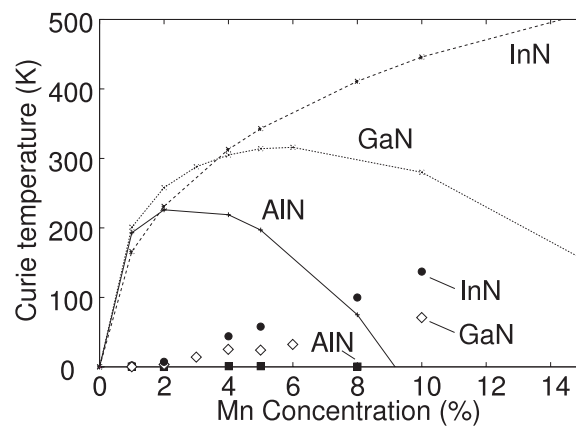
**Figure 1.** Effective exchange interactions in (a) (Al, Mn)N, (b) (Ga, Mn)N, (c) (In, Mn)N and (d) (Ga, Mn)As in the ferromagnetic state.

Figure 3 shows the  $T_C$  for (Al, Mn)N, (Ga, Mn)N and (In, Mn)N calculated by using the mean field approximation (MFA) and Monte Carlo simulation (MCS). In principle, the MCS gives the exact  $T_C$  within the statistical error. In (Al, Mn)N, (Ga, Mn)N and (In, Mn)N, the  $T_C$  calculated using the MFA are approximately proportional to  $\sqrt{c}$  for low concentrations. This is a typical concentration dependence for  $T_C$  in double-exchange systems [25, 26]. The saturation of  $T_C$  in (Al, Mn)N and (Ga, Mn)N for high concentrations is due to the antiferromagnetic superexchange between the Mn. In the (In, Mn)N,  $T_C$  reaches up to 200 K for 15% of Mn.

Comparison of the MFA values to exact MCS values reveals that the MFA significantly overestimates  $T_C$  for DMS. In particular, according to the MCS predictions (Al, Mn)N is practically paramagnetic for the concentrations investigated and  $T_C$  is very low for (Ga, Mn)N and (In, Mn)N for low concentrations. This strong reduction of  $T_C$  in the MCS calculations is explained from the viewpoint of magnetic percolation [5, 6]. As shown in figures 1(a)–(c), in nitride DMS only the first- and the fourth-neighbour interactions make a meaningful contribution to the ferromagnetism. By analogy with the percolation problem, it is intuitively understood that we cannot expect ferromagnetic order below the percolation threshold. In the present case of the FCC structure, the percolation threshold for nearest neighbour interactions is 20% [27] and it is much higher than typical experimental concentrations (about 10% or less). Below the threshold, the system shows a paramagnetic state or ferromagnetic state with low  $T_C$  with distant weak interactions. This is why we find very low  $T_C$  in nitride DMS for low concentrations. The experimental values are well reproduced by the MCS calculations in particular for (Ga, Mn)P, (Ga, Mn)As and (Zn, Cr)Te in figure 4, except for the very high  $T_C$  values observed in (Ga, Mn)N, (Ga, Mn)P and (Ga, Cr)N.



**Figure 2.** Total (solid lines) and partial (dotted lines) densities of states in (a) (Al, Mn)N, (b) (Ga, Mn)N, (c) (In, Mn)N and (d) (Ga, Mn)As in the ferromagnetic state.



**Figure 3.** Curie temperatures of (Al, Mn)N, (Ga, Mn)N and (In, Mn)N as a function of magnetic impurity concentration. Curie temperatures are calculated by using the mean field approximation (MFA, plotted by lines), and the Monte Carlo simulation (MCS, indicated by symbols).

### 3. Spinodal decomposition and its application

As shown in the previous section, we have succeeded in reproducing experimental  $T_C$  for (Ga, Mn)P, (Ga, Mn)As and (Zn, Cr)Te accurately from first principles. In contrast to this success, agreement between the theory and experiments is not satisfactory for wide band

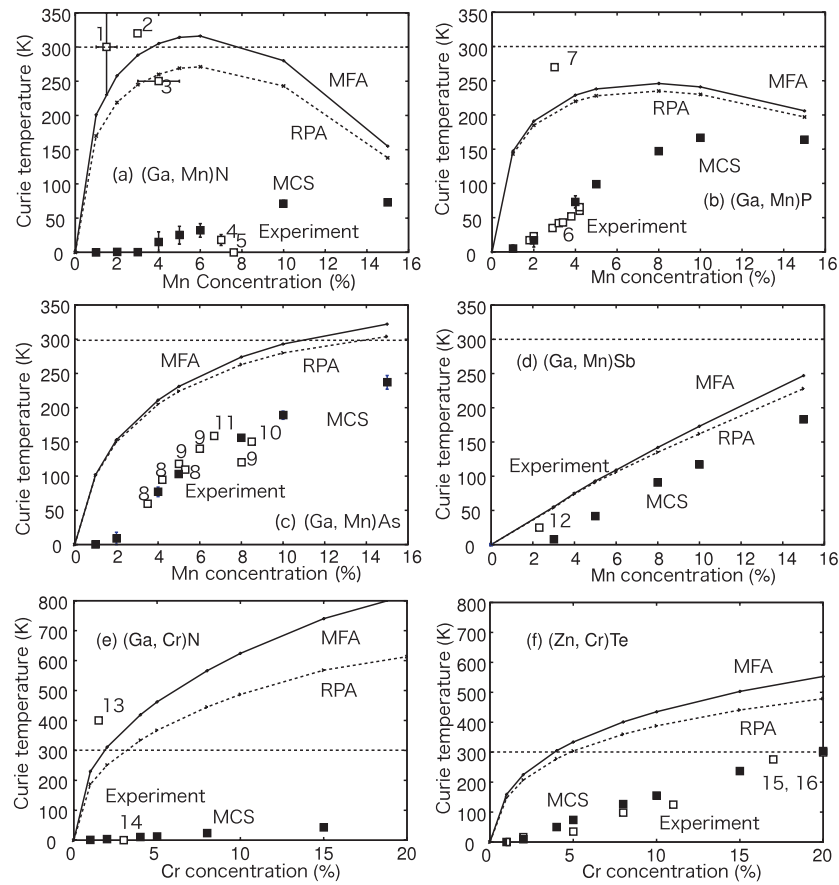


**Figure 4.** Curie temperatures of (a) (Ga, Mn)N, (b) (Ga, Mn)P, (c) (Ga, Mn)As, (d) (Ga, Mn)Sb, (e) (Ga, Cr)N and (f) (Zn, Cr)Te as a function of magnetic impurity concentration. Curie temperatures are calculated by using the mean field approximation (MFA, solid lines), the random phase approximation (RPA, dotted lines) and the Monte Carlo simulation (MCS, filled squares). Available experimental values [28] are also shown (open squares).

gap DMS such as nitride DMS, and a more realistic description of wide band gap DMS is needed. For example, in general, DMS systems have a solubility gap and in thermal equilibrium they show phase separation (spinodal decomposition); however in the previous theoretical approaches homogeneous impurity distribution is supposed. In this section we focus on the spinodal decomposition in nitride DMS, such as (Ga, Mn)N and (Ga, Cr)N, and study how inhomogeneous impurity distribution affects the ferromagnetism. The spinodal decomposition of DMS is simulated by applying the Monte Carlo method for the Ising model with the calculated pair interactions. Curie temperatures of simulated spinodal decomposition phases are calculated within the random phase approximation, taking disorder into account [8, 9].

In figure 5, simulation results are summarized. Figure 5(a) shows the initial random configuration of (Ga, Cr)N. Due to the attractive interactions, (Ga, Cr)N shows phase separation (figure 5(b)). For the concentration investigated, 5%, the system is superparamagnetic ( $T_C = 0$ ) because small isolated clusters are formed in DMS due to the decomposition (Dairiseki phase). For higher concentrations, it is found that the spinodal decomposition helps to make a magnetic

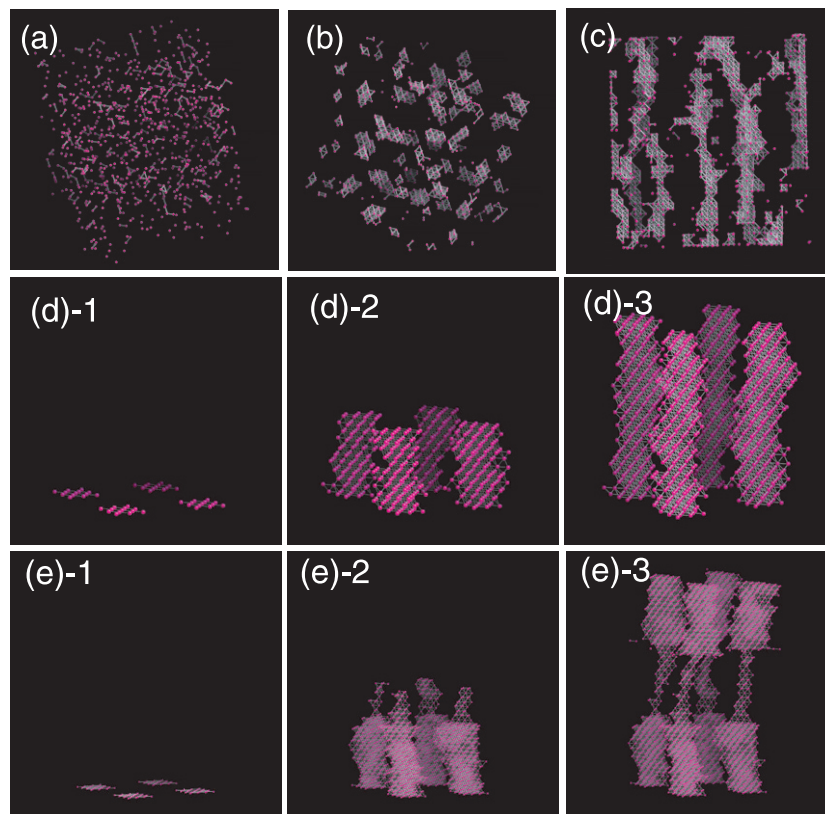


**Figure 5.** Monte Carlo simulation of spinodal decomposition in DMS. Transition metal impurities in DMS are shown by dots and nearest neighbour pairs are connected by lines. (a) Initial random configuration of Cr in (Ga, Cr)N, (b) Dairiseki phase (3D spinodal nanodecomposition) in (Ga, Cr)N, (c) Konbu phase (2D spinodal nanodecomposition) in (Ga, Cr)N, (d) nanomagnets formed in (Zn, Cr)Te by 2D spinodal decomposition with seeding and (e) shape control of the Konbu phase in (Zn, Cr)Te.

(This figure is in colour only in the electronic version)

network in the DMS and raise  $T_C$  above room temperature [8]. However, this effect is remarkable only for the concentrations above the nearest neighbour percolation threshold and does not explain the high  $T_C$  phase which was observed experimentally for low concentrations.

In the actual experiments, a non-equilibrium crystal growth technique, such as MBE or MOCVD, is used to fabricate DMS. In these methods, atomic materials are deposited layer by layer. We can introduce the layer-by-layer condition into our simulations for spinodal decomposition, i.e., after annealing the first layer we fix the resulting configuration of the first layer and deposit the second layer. The annealing simulation is only performed for the second layer. By repeating this process we simulate the spinodal decomposition under the layer-by-layer crystal growth condition. Due to the attractive interactions between impurities, magnetic impurities in the second layer favour being just on the clusters formed in the first layer. Thus, by introducing a layer-by-layer condition in our simulations, finally a quasi-one-dimensional nanostructure (Konbu phase) [9] of impurities is formed in DMS. Our simulations show that rather large nanomagnets can be formed even for low concentrations as shown in figure 5(c). In this case, the superparamagnetic blocking effect plays an important role in the magnetization



process. The Monte Carlo simulation for the magnetization process of the decomposition phases indicates that the superparamagnetic blocking temperature could be higher because the activation energy for flipping the magnetization becomes larger for the decomposition phases.

We can use the formation of Konbu phases in DMS as a novel technique for fabricating semiconductor spintronics devices. For example, as shown in figure 5(d), by the Monte Carlo simulation we have shown that we can specify the position of nanostructures in the Konbu phase by putting seeds at desired positions (figure 5(d)-1) before the MBE process. The nanomagnets are formed just at the seeding position (figures 5(d)-2, 3). Moreover, by controlling the impurity concentration during MBE growth, we can control the shape of the nanostructures as shown in figure 5(e). These simulations suggest a new way to fabricate 100 Tbit density of a nanomagnet array with controlled shape.

#### 4. Summary

We have discussed ferromagnetism of nitride DMS based on first-principles calculations by the KKR-CPA method.  $T_C$  values for the DMS are calculated by using the Monte Carlo method for the classical Heisenberg model with realistic exchange interactions calculated from first principles. It is found that the  $T_C$  values of nitride DMS are very low since, due to short ranged interaction, percolation of the ferromagnetic coupling is difficult to achieve for low concentrations. The calculated  $T_C$  values for homogeneous DMS in II–VI and III–V such as (Ga, Mn)P, (Ga, Mn)As and (Zn, Cr)Te by MCS agree very well with available experimental values. The three-dimensional (3D) spinodal nanodecomposition is simulated by applying the MCS to the Ising model with *ab initio* chemical pair interactions between magnetic impurities in DMS. It is found that the 3D *Dairiseki phase* inherently occurs in DMS due to strong attractive interactions between the magnetic impurities. We design a two-dimensional spinodal nanodecomposition under the layer-by-layer crystal growth condition, leading to characteristic quasi-one-dimensional nanostructures named the 1D *Konbu phase* in DMS. The blocking phenomena in the superparamagnetism, the magnetic dipole–dipole interaction, and the 3D network of the one-dimensional structures should be considered for high  $T_C$  DMS. We design a new crystal growth method of positioning by a seeding and shape controlling method in 100 Tbit density for nanomagnets in the semiconductor matrix with a high blocking temperature.

#### Acknowledgments

This research was partially supported by a Grant-in-Aid for Scientific Research in Priority Areas ‘Quantum Simulators and Quantum Design’ (No. 17064014) and ‘Semiconductor Nanospintronics’, a Grand-in-Aid for Scientific Research for young researchers, JST-CREST, NEDO-nanotech, the 21st Century COE and the JSPS core-to-core programme ‘Computational Nanomaterials Design’. This research was also supported in part by the National Science Foundation under Grant No. PHY99-07949 (KITP SPINTRONICS05 programme in UCSB).

#### References

- [1] Wolf S A *et al* 2001 *Science* **294** 1488
- [2] Sato K and Katayama-Yoshida H 2002 *Semicond. Sci. Technol.* **17** 367
- [3] Dietl T 2002 *Semicond. Sci. Technol.* **17** 377
- [4] Sato K, Dederichs P H and Katayama-Yoshida H 2003 *Europhys. Lett.* **61** 403
- [5] Bergqvist L, Eriksson O, Kudrnovský J, Drchal V, Korzhavyi P and Turek I 2004 *Phys. Rev. Lett.* **93** 137202



- [6] Sato K, Schweika W, Dederichs P H and Katayama-Yoshida H 2004 *Phys. Rev. B* **70** 201202(R)
- [7] Fukushima T, Sato K and Katayama-Yoshida H 2004 *Japan. J. Appl. Phys.* **43** L1416
- [8] Sato K, Katayama-Yoshida H and Dederichs P H 2005 *Japan. J. Appl. Phys.* **44** L948
- [9] Fukushima T, Sato K, Katayama-Yoshida H and Dederichs P H 2006 *Japan. J. Appl. Phys.* **45** L416
- [10] Bouzerar G, Ziman T and Kudrnovský J 2005 *Europhys. Lett.* **69** 812
- [11] Hilbert S and Nolting W 2005 *Phys. Rev. B* **71** 113204
- [12] Akai H and Dederichs P H 1993 *Phys. Rev. B* **47** 8739
- [13] Akai H 2002 <http://sham.phys.sci.osaka-u.ac.jp/kkr/>
- [14] Liechtenstein A I, Katsnelson M I, Antropov V P and Gubanov V A 1987 *J. Magn. Magn. Mater.* **67** 65
- [15] Pajda M, Kudrnovský J, Turek I, Drchal V and Bruno P 2001 *Phys. Rev. B* **64** 174402
- [16] Bouzerar G, Kudrnovský J, Bergqvist L and Bruno P 2003 *Phys. Rev. B* **68** 81203(R)
- [17] Bergqvist L, Korzhavyi P A, Sanyal B, Mirbt S, Abrikosov I A, Nordström L, Smirnova E A, Mohn P, Svedlindh P and Eriksson O 2003 *Phys. Rev. B* **67** 205201
- [18] Bergqvist L, Eriksson O, Kudrnovský J, Drchal V, Bergman A, Nordström L and Turek I 2005 *Phys. Rev. B* **72** 195210
- [19] Kudrnovský J, Drchal V, Turek I, Bergqvist L, Eriksson O, Bouzerar G, Sandratskii L and Bruno P 2004 *J. Phys.: Condens. Matter* **16** S5571
- [20] Iusan D, Sanyal B and Eriksson O 2006 *Phys. Rev. B* **74** 235208
- [21] Ležaić M, Mavropoulos Ph, Enkovaara J, Bihlmayer G and Bluegel S 2006 *Phys. Rev. Lett.* **97** 26404
- [22] Sanyal B, Bergqvist L and Eriksson O 2003 *Phys. Rev. B* **68** 54417
- [23] Wyckoff R W G 1963 *Crystal Structures* 2nd edn, vol 1 (New York: Wiley) p 111
- [24] Kanamori J and Terakura K 2001 *J. Phys. Soc. Japan* **70** 1433
- [25] Akai H 1998 *Phys. Rev. Lett.* **81** 3002
- [26] Sato K, Dederichs P H, Katayama-Yoshida H and Kudrnovský J 2004 *J. Phys.: Condens. Matter* **16** S5491
- [27] Stauffer D and Aharony A 1994 *Introduction to Percolation Theory* revised 2nd edn (London: Taylor and Francis)
- [28] Reed M L *et al* 2001 *Appl. Phys. Lett.* **79** 3473
- Thaler G T *et al* 2002 *Appl. Phys. Lett.* **80** 3964
- Theodoropoulou N *et al* 2001 *Appl. Phys. Lett.* **78** 3475
- Overberg M E *et al* 2001 *Appl. Phys. Lett.* **79** 1312
- Ploog K H *et al* 2003 *J. Vac. Sci. Technol. B* **21** 1756
- Matsukura F *et al* 1998 *Phys. Rev. B* **57** R2037
- Edmonds K W *et al* 2002 *Appl. Phys. Lett.* **81** 4991
- Ku K C *et al* 1993 *Appl. Phys. Lett.* **82** 2302
- Edmonds K W *et al* 2004 *Phys. Rev. Lett.* **92** 37201
- Hashimoto M *et al* 2003 *J. Cryst. Growth* **251** 327
- Yamaguchi K *et al* 2004 *Japan. J. Appl. Phys.* **43** L1312
- Saito H *et al* 2003 *Phys. Rev. Lett.* **90** 207202
- Ozaki N *et al* 2004 *Phys. Status Solidi* **1** 957